26 May 2010, 4:45 pm - 6:45 pm

Computational Modeling of a Large Pile Group Under Lateral Load

Jinchi Lu
University of California, San Diego, La Jolla, CA

Ahmed Elgamal
University of California, San Diego, La Jolla, CA

Charles Sikorsky
CALTRANS, Sacramento, CA

Thomas Shantz
CALTRANS, Sacramento, CA

Fifth International Conference on
Recent Advances in Geotechnical Earthquake Engineering and Soil Dynamics
and Symposium in Honor of Professor I.M. Idriss
May 24-29, 2010 • San Diego, California

COMPUTATIONAL MODELING OF A LARGE PILE GROUP UNDER LATERAL LOAD

Jinchi Lu
Univ. of California, San Diego
La Jolla, CA 92093

Ahmed Elgamal
Univ. of California, San Diego
La Jolla, CA 92093

Charles Sikorsky
CALTRANS
Sacramento, CA 95816

Thomas Shantz
CALTRANS
Sacramento, CA 95819

ABSTRACT

The lateral load resistance of pile foundations is critically important to the design of structures that may be subjected to earthquakes. This paper presents computational modeling results of the response of a large pile group system under lateral load. The open-source platform OpenSees is employed to conduct a nonlinear 3-dimensional finite element analysis. The piles are modeled by beam-column elements, and rigid beam-column elements are used to model the pile size (diameter). In order to facilitate the pre- and post-processing phases, a recently developed user interface OpenSeesPL is employed. Distribution of load within the pile group is presented and the group interaction effects are discussed. Under lateral loading, corner piles shoulder the greatest burden in resisting the resulting shear, bending, and axial loads. Lower compressive or even tensile axial forces in the back piles may greatly weaken/deteriorate the structural reinforced concrete properties. Further validation and calibration of the analysis framework may be conducted with the aid of case histories and experimental data.

INTRODUCTION

Soil-structure interaction (SSI) plays a major role in the lateral response of structures to earthquakes. In order to satisfactorily reproduce these SSI effects computationally, it is often necessary to model a large domain of the soil surrounding the structure of interest. High spatial/temporal resolution is another challenge in analyzing such models. With the developments in material modeling techniques and high-speed efficient computers, linear and nonlinear three-dimensional (3D) finite-element (FE) methods are becoming a promising technique for understanding the involved SSI mechanisms. Particularly suited to seismic applications, the open-source computational platform OpenSees (Mazzoni et al. 2006) provides such 3D simulation capabilities.

This paper presents a pilot 3D FE study of a large pile group system under lateral loading. The open-source platform OpenSees (Mazzoni et al. 2006) is employed to conduct the FE analysis. In order to facilitate the pre- and post-processing phases, a recently developed user interface OpenSeesPL (Figs. 1 and 2) is employed. OpenSeesPL allows for the execution of push-over and seismic pile-ground simulations (Lu et al. 2006, http://cyclic.ucsd.edu/openseespl/). Various ground modification scenarios may be also studied by appropriate specification of the material within the pile zone.

In the following sections, an overview of OpenSeesPL capabilities is first presented, followed by pushover analysis of a pile group system (conducted with the aid of OpenSeesPL). For comparison, a representative single-pile reference simulation is also studied. Along with the insights gained from these studies, the reported effort aims to highlight the analysis framework capabilities and range of potential applications. Further refinement and calibration of this framework will result in higher fidelity and more insightful outcomes.

COMPUTATIONAL FRAMEWORK

The open-source platform OpenSees (http://opensees.berkeley.edu, Mazzoni et al. 2006) is employed throughout. OpenSees is a software framework for developing applications to simulate the performance of structural and geotechnical systems subjected to dynamic earthquake excitation.

In the OpenSees platform, a wide range of linear and nonlinear soil and structural elements is available. The reported pre- and post-processing scenarios are generated by the user interface OpenSeesPL which allows for (Figs 1 and 2): i) convenient generation of the mesh (surface load/footing, single pile, and pile group), associated boundary conditions, and loading parameters (FE input file), ii) execution of the computations using the OpenSees platform, and iii) graphical display of the results for the footing/pile and the ground system.

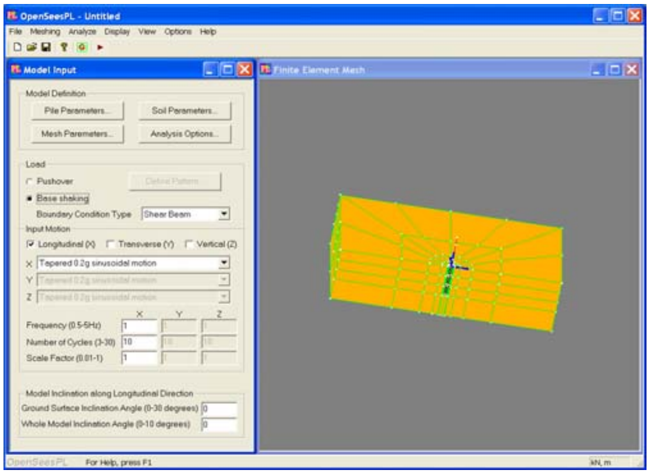

Fig. 1. OpenSeesPL user interface with mesh showing a circular pile in level ground (Lu et al. 2006).

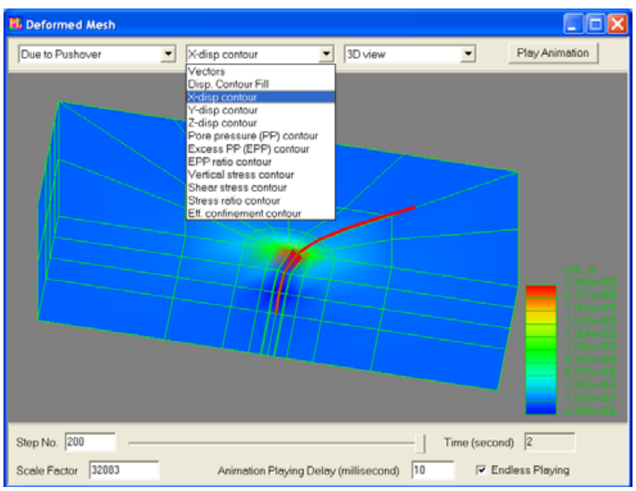

Fig. 2. Push-over analysis and deformed mesh window in OpenSeesPL (Lu et al. 2006).

PRE- & POST-PROCESSING

The OpenSeesPL graphical interface (pre- and post-processor) is focused on facilitating a wide class of 3D studies (with additional capabilities yet under development). In the current version, OpenSeesPL may be employed to study a number of geometries and configurations of interest including:

i) Linear and nonlinear (incremental-plasticity based) 3D ground seismic response with capabilities for 3D excitation, and layered soil strata. Multi-yield surface cohesionless (Drucker-Prager cone model), and cohesive (Mises or J_2) soil models are available (Elgamal et al. 2003; Yang et al. 2003). The available coupled solid-fluid analysis option allows for conducting liquefaction studies.

ii) Inclusion of a pile or pile group in the above-described 3D ground mesh (circular or square pile in a soil island). For the pile response, linear, bilinear elastic-plastic, or nonlinear fiber elements are available in OpenSees (Mazzoni et al. 2006). The pile may extend above ground, and may support a bridge deck or a point mass at the top. This bridge deck can be specified to only translate longitudinally, or to undergo both lateral translation and transversal rotation. In addition to the seismic excitation option, the pile system may be subjected to monotonic or cyclic lateral push-over loading (in prescribed displacement, or prescribed force modes).

iii) Soil properties within the zone occupied by the pile (as dictated by pile diameter) can be specified independently, allowing for a variety of practical modeling situations. For instance, various ground modification scenarios may be studied by appropriate specification of the material within the pile zone. Among other options, liquefaction countermeasures in the form of gravel drains, stone columns, and solidification/cementation may all be analyzed. Of particular importance and significance in these scenarios is the ability to simulate the presence of a mild infinite-slope configuration, allowing estimates of accumulated ground deformation, efficacy of a deployed liquefaction countermeasure, pile-pinning effects, and liquefaction-induced lateral pile loads and resulting moments/stresses (Elgamal et al. 2009).

iv) Piles embedded in a mildly sloping ground can also be simulated within this interface.

In addition, OpenSeesPL allows convenient post-processing and graphical visualization of the analysis results including the deformed mesh (Fig. 2), ground response time histories, and pile response. As such, OpenSeesPL makes it possible for geotechnical and structural engineers/researchers to rapidly build a model, run the FE analysis, and evaluate performance of the pile-ground system (Lu et al. 2006).

PILE GROUP

A model that is representative of salient characteristics of the Dumbarton Bridge (California) Pier 23 pile-group foundation was studied. The pile group is configured in an 8 x 4 arrangement with a longitudinal spacing of 2 pile diameters and a transversal spacing of 2.15 pile diameters on center. Each pile is 1.37 m in diameter and 30.8 m long. The group is rigidly connected by a pile cap 14.3 m above the mudline. A vertical load of 28,900 kN was estimated to represent the tributary own weight of the bridge deck.

<u>Pile Properties</u>

Concrete-in-filled pre-stressed pipe piles were used, with a wall thickness h = 0.1778 m. The bending stiffness for each pile was modeled as $EI = 2 \times 10^7$ kN-m^2 (pile response is assumed to remain linear).

Soil Profile

Three soil layers were employed (Table 1). As modeled in this study, the upper 2 layers were 6.7 m each in thickness and the bottom layer had a thickness of 30.5 m. The pressure-independent (J_2) multi-yield surface plasticity model was employed in which a hyperbolic relationship describes the shear stress-strain backbone curve. A Poisson's ratio of 0.4 was specified for all layers.

Table 1. Soil Material Properties

Material Property	Top layer	Middle layer	Bottom layer
Mass density (ton/m^3)	1.3	1.5	1.8
Shear wave vel. (m/s)	122	152	183
Shear modulus (MPa)	19.3	34.7	60.3
Shear strength (kPa) occurring at a specified shear strain γ_{max} = 3%	34	58	75

Finite Element Model

In view of symmetry, a half mesh configuration is used (Fig. 3). Length of the mesh in the longitudinal direction is 394 m, with 191 m transversally (in this half-mesh configuration, resulting in a 394 m x 382m soil domain in plan view). Total layer thickness is 43.9 m (the base of the soil domain is 27.4 m below the pile tip). The soil domain is modeled by eight-node brick elements (23,040 in total) and the piles are modeled by beam-column elements (512 in total). As mentioned earlier, rigid beam-column elements (1,664 in total) are used around each pile to model the pile size (diameter).

In the employed ½ mesh of Fig. 3 (due to symmetry), the following boundary conditions were enforced: i) The bottom of the domain is fixed in the longitudinal (X), transverse (Y), and vertical (Z) directions., b) Left, right and back planes of the mesh are fixed in X and Y directions (the lateral directions) and free in the Z direction, and iii) In this half mesh configuration, the plane of symmetry is fixed in Y and free in Z and X direction (to model the full-mesh 3D scenario).

Specified Load

Due to symmetry, half of the vertical dead load (-14,450 kN) was imposed initially (after imposing the soil domain own weight). Thereafter, a pile cap longitudinal displacement was applied up to a maximum of 0.12 m (allowing the final lateral load to exceed the applied vertical bridge own-weight force).

Summary of Main Results

Overall Response Fig. 4 shows lateral load versus displacement for the entire pile group at the pile cap elevation (this load is equal to the sum of the shear forces across all 32 piles at the pile cap). A load of 29,194 kN (representative of the full mesh configuration) is reached at the pile cap longitudinal displacement of 0.12 m. Compared to the single pile scenario (see Single Pile section below), it may be concluded that the pile group efficiency (lateral resistance of the pile group versus that of the single pile at equal levels of final deflection) for this case is 29194 / (2637 x 32) = 0.35.

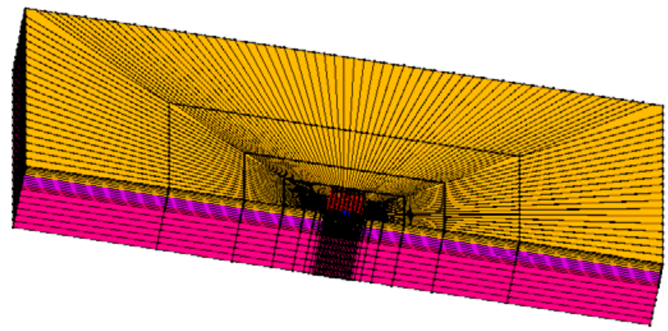

a)

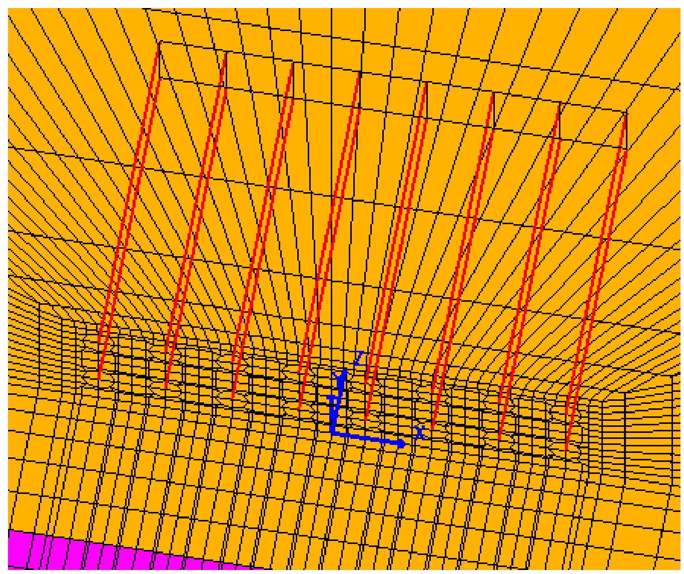

b)

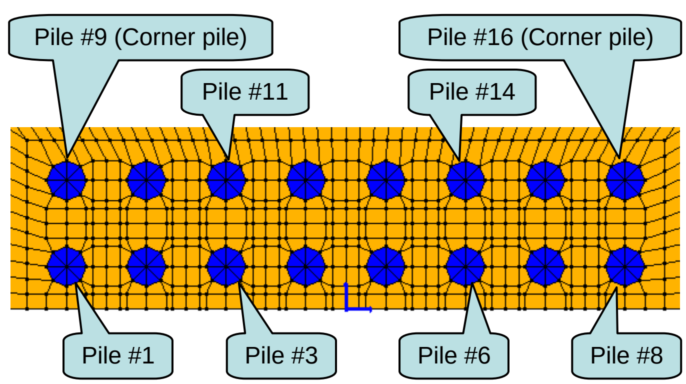

c)

Fig. 3. Finite element mesh: a) isometric view; b) close-up of pile group; c) pile group layout (back piles are 1 and 9 and front piles are 8 and 16).

Final Deformed Mesh The final deformed mesh in shown in Fig. 5a, along with the stress ratio contour fill (red color shows yielded soil elements). Fig. 5b displays the deformed mesh of the pile group skeleton only. Along with translation, the pile group is seen to also undergo some overall rotation.

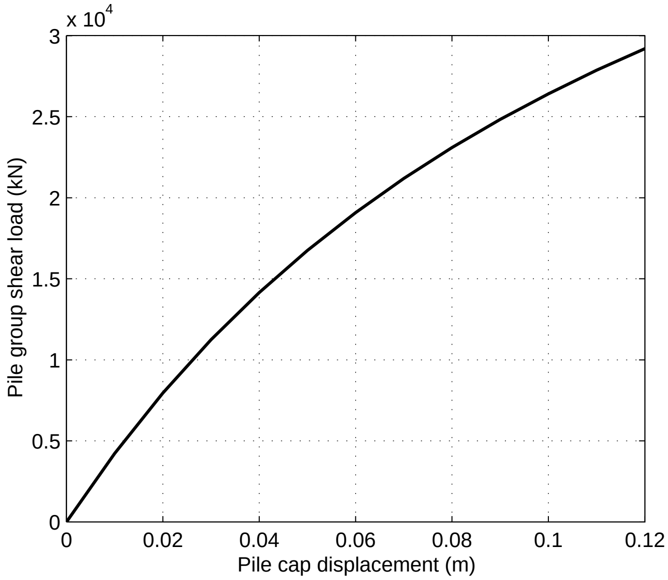

Fig. 4. Lateral (longitudinal) shear load versus displacement curve for pile group.

Load Distribution At the 0.12 m pile cap longitudinal displacement, the corresponding shear force and bending moment distribution between piles in the pile group is shown in Table 2. The corner front pile (Pile #16) carries the highest portion of shear force and bending moment. The center front pile (pile # 8), and the two back piles (#s 1 and 9) also sustain relatively high levels of load. The inner piles (#s 3-6) carry the least burden (about 60% of the share of pile # 16).

Response Profiles At the 0.12m pile cap longitudinal displacement, the response profiles for the front piles (Piles #8 and #16) are shown in Fig. 6. Essentially, piles #8 and #16 behave in a similar fashion, with the corner front pile (Pile #16) carrying noticeably larger shear and axial loads. For pile # 16, the resulting peak longitudinal moment is 13,010 kN-m at the pile cap and -6,440 kN-m (at 6.7 m below the mudline).

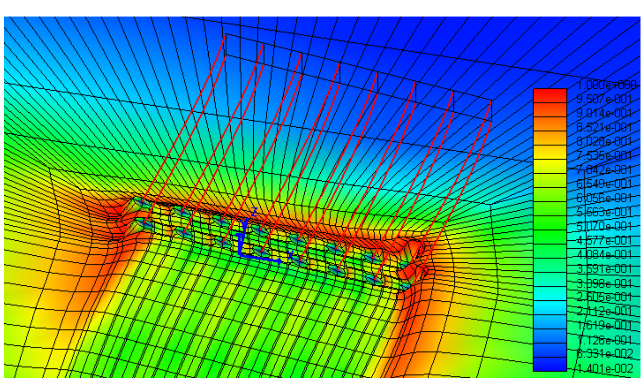

a)

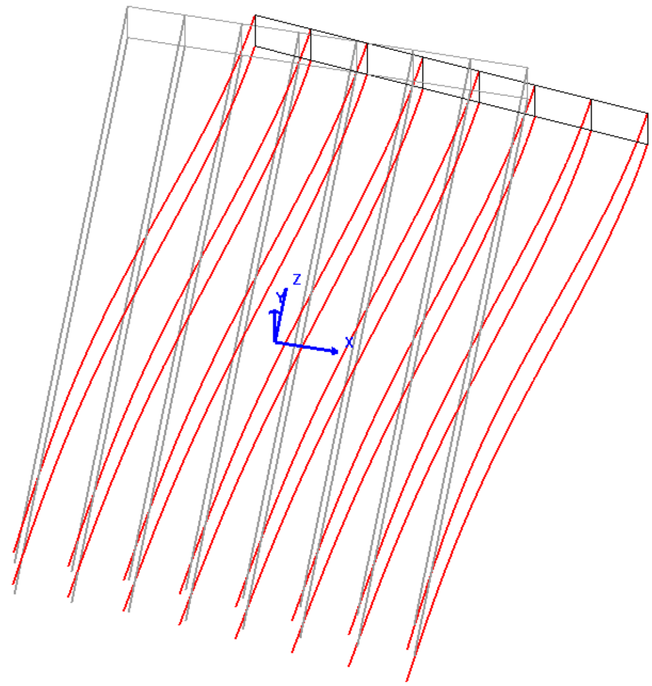

b)

Fig. 5. Final deformed mesh (factor of 50): a) stress ratio contour fill (red color shows yielded soil elements); b) pile group (gray lines show the undeformed mesh).

Table 2. Load distribution by pile for pile-cap longitudinal displacement at 0.12 m

Pile #	V_{Long} (kN)	Ratio	M_{Long} (kN-m)	Ratio
1	-986.8	6.8%	11440	6.6%
2	-849	5.8%	10320	6.0%
3	-784.4	5.4%	9760	5.6%
4	-756.3	5.2%	9508	5.5%
5	-756.9	5.2%	9505	5.5%
6	-787.7	5.4%	9764	5.6%
7	-857.8	5.9%	10360	6.0%
8	-1005	6.9%	11580	6.7%
9	-1163	8.0%	12920	7.5%
10	-975.4	6.7%	11420	6.6%
11	-899.5	6.2%	10780	6.2%
12	-866.9	5.9%	10490	6.1%
13	-865.2	5.9%	10460	6.0%
14	-895.5	6.1%	10710	6.2%
15	-971.1	6.7%	11350	6.5%
16	-1176	8.1%	13010	7.5%
Total	**-14597**	**100%**	**1.73E+05**	**100%**

Fig. 7 shows the corresponding response profiles of the back piles (#1 and #9). The back corner pile (Pile #9) experiences the highest tensile axial force (2,900 kN). The peak longitudinal moment is 12,920 kN-m at the pile cap and -6,226 kN-m (at 4.9 m below the mudline), and the peak longitudinal shear is 1,163 kN. Compared to pile # 1, the corner back pile (#9) carries a slightly higher shear force and a significantly larger axial load (in tension).

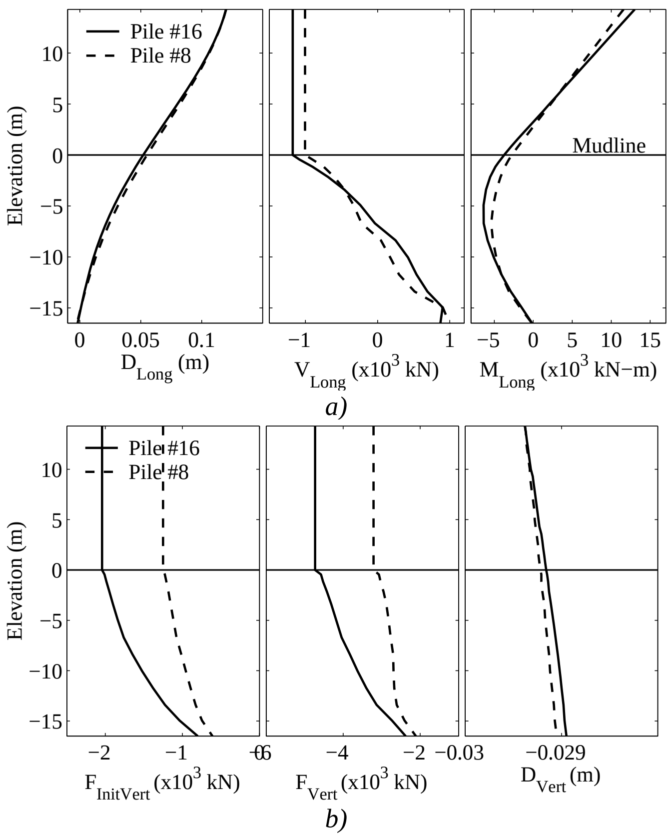

Fig. 6. Response profiles of front piles (see Fig. 3 for pile group layout; D_{Long}: longitudinal displacement; V_{Long}: longitudinal shear force; M_{Long}: bending moment in the longitudinal plane; $F_{InitVert}$: axial force due to gravity; F_{Vert}: axial force; D_{Vert}: vertical displacement).

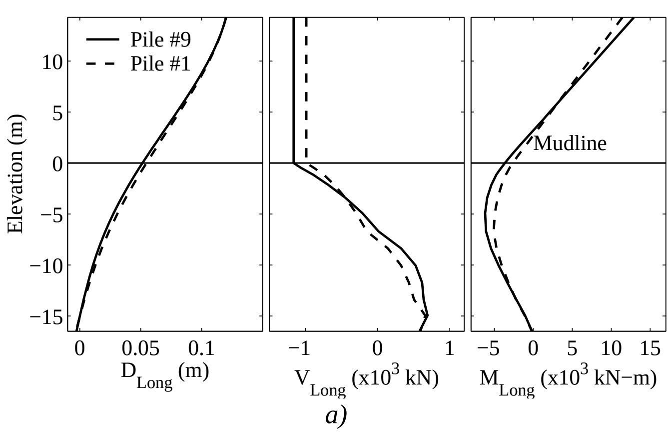

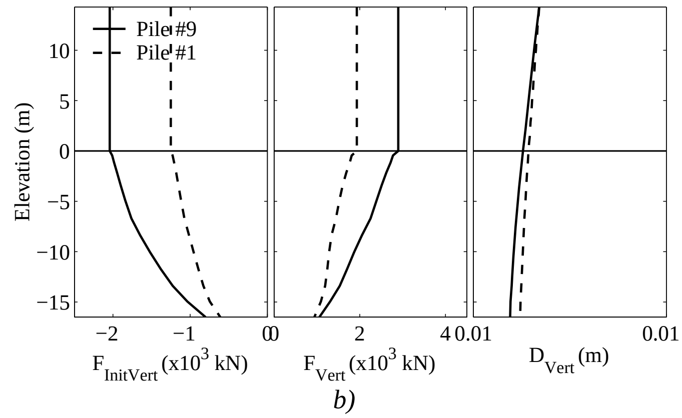

Fig. 7. Response profiles of back piles (see Fig. 3 for pile group layout; D_{Long}: longitudinal displacement; V_{Long}: longitudinal shear force; M_{Long}: bending moment in the longitudinal plane; $F_{InitVert}$: axial force due to gravity; F_{Vert}: axial force; D_{Vert}: vertical displacement).

<u>Loading History</u>

The pile cap displacement of 0.12 m was applied in 12 steps. Response profiles of the pile experiencing the highest moment and shear (the corner front pile #16, Fig. 3) are shown in Fig. 8. Below the mudline, maximum moment and shear location is seen to propagate downwards with the level of applied lateral deformation (due to soil yielding at the upper layers of the stratum).

<u>Axial Force Distribution</u>

The axial force distribution between piles in the pile group is shown in Table 3 (along with the initial dead load counterpart). Even in the initial static state, the share of each pile varies in a wide range. Piles along the circumference carry most of the load with the corner piles shoulder the biggest burden. The inner piles (#s 2-7) hardly see much of the applied dead load.

At the prescribed 0.12m longitudinal pile cap displacement, the compressive axial forces increase dramatically in the front piles (#s 4-8 and 12-16). Conversely, the back piles experience tensile forces reaching a maximum of about 2900 kN in the back corner pile # 9.

Figs. 9-112 display the axial force load history profiles for selected piles. In each figure, similarly located front and back pile responses are compared. Compressive forces are seen to gradually increase in the front piles, while the back piles eventually experience substantial tensile axial forces. Evolution of axial load transfer mechanism from the pile to the surrounding soil during the loading process may be also observed.

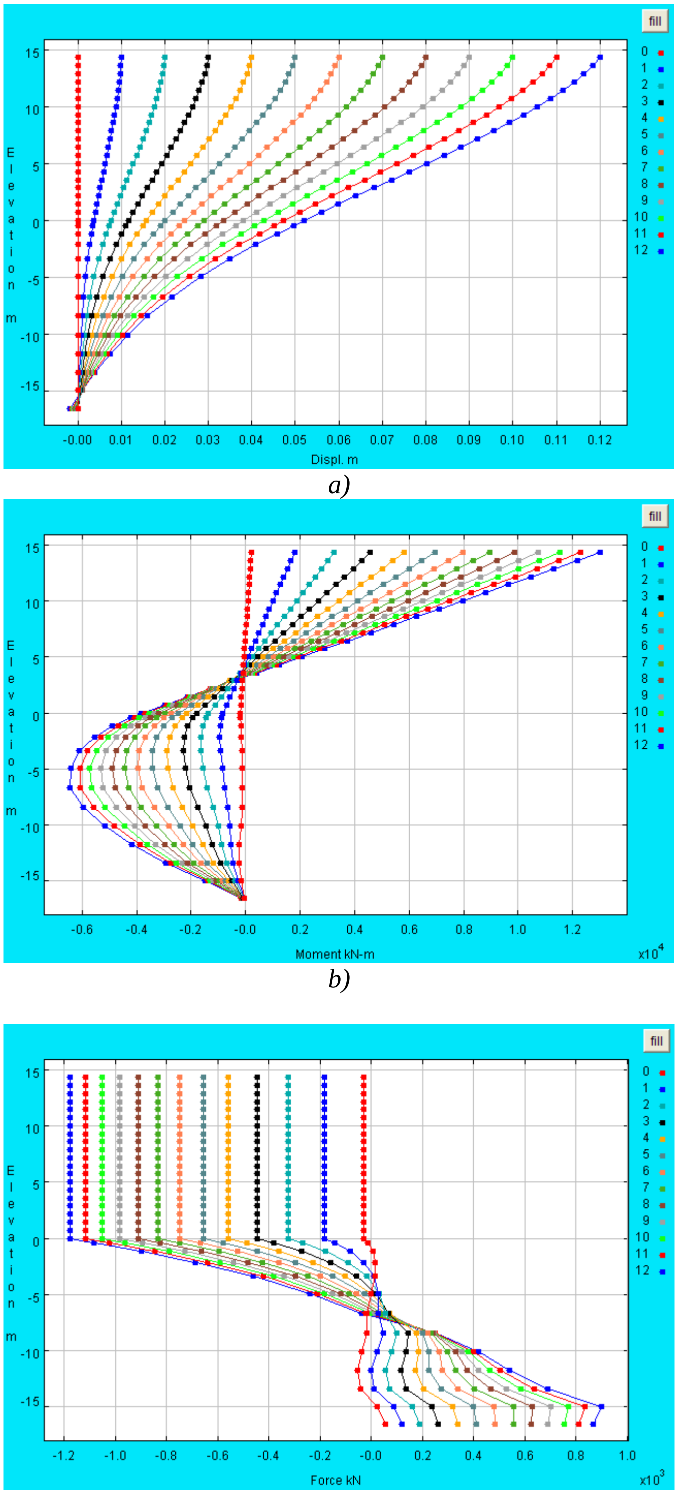

a) b) c)

Fig. 8. Response profiles for Pile #16 (see Fig. 3c for pile group layout): a) longitudinal displacement; b) longitudinal bending moment; c) longitudinal shear force.

Table 3. Axial force distribution by pile for pile-cap longitudinal displacement at 0.12 m (and the initial dead load counterpart).

Pile #	F_{Vert} (kN)	F_{Vert}/F_{vertS}*	$F_{InitVert}$ (kN)	$F_{InitVert}/F_{vertS}$*
1	1933	-2.1	-1251	1.4
2	418.6	-0.5	-378.2	0.4
3	8.995	-0.0	-269.4	0.3
4	-400.9	0.4	-251.4	0.3
5	-699.1	0.8	-251.4	0.3
6	-938	1.0	-269.5	0.3
7	-1244	1.4	-378.2	0.4
8	-3211	3.6	-1251	1.4
9	2899	-3.2	-2042	2.3
10	719.5	-0.8	-1140	1.3
11	-389.8	0.4	-969.1	1.1
12	-1315	1.5	-923.6	1.0
13	-1984	2.2	-923.6	1.0
14	-2503	2.8	-969	1.1
15	-3016	3.3	-1140	1.3
16	-4728	5.2	-2042	2.3
Total	**-14450**		**-14450**	

* F_{vertS} is the single pile dead load (F_{vertS} = -903.5 kN)

REPRESENTATIVE SINGLE PILE REFERENCE SIMULATION

For comparison, a single fixed head pile was also studied. The geometrical and material properties of this pile are identical to those of any of the piles in the pile group. The imposed dead load was -903.5 kN (= -28900 kN / 32 piles). The pile cap longitudinal displacement was applied up to 0.12 m.

A half mesh configuration was used (Fig. 13). Length of the mesh in the longitudinal direction is 192 m, with 96 m transversally (in this half-mesh configuration, resulting in a 192 m x 192 m soil domain simulation in plan view). The soil layer thickness (43.9 m) and properties are the same as those of the pile group case (the bottom of the soil domain is 27.4 m below the pile tip). Half of the dead load (-451.75 kN) was applied in this half mesh configuration due to symmetry.

<u>Summary of Main Results</u>

<u>Overall response</u> Fig. 14 shows the lateral load versus pile head displacement. A lateral load of 2,637 kN (representative of the full mesh configuration) was reached at the pile head longitudinal displacement of 0.12 m.

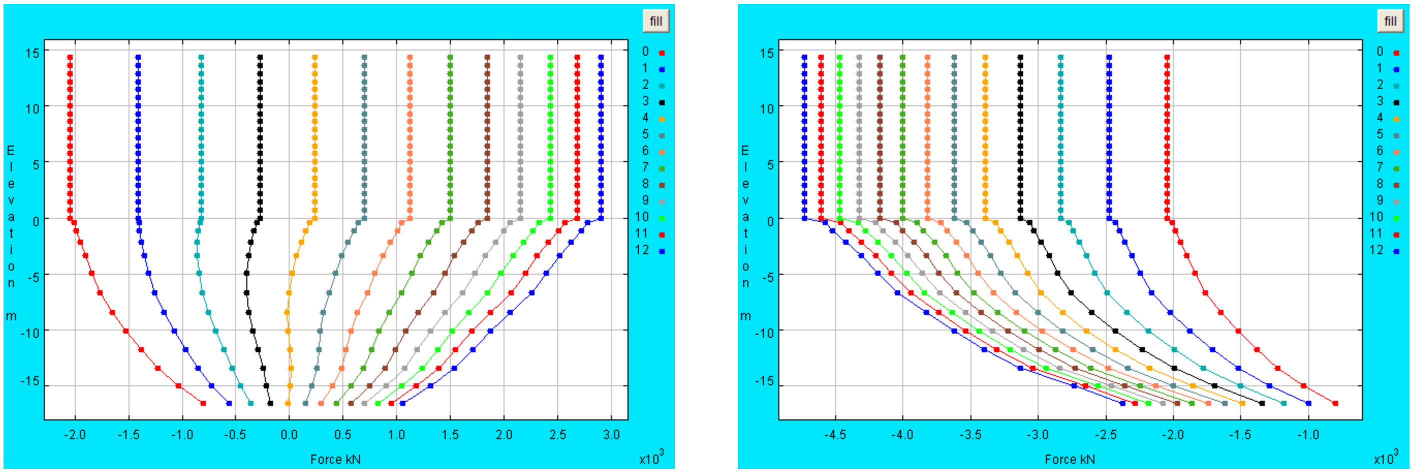

(a) (b)

Fig. 9. Axial force profile: a) Corner Pile # 9, and b) Corner Pile # 16 (see Fig. 3c for pile group layout).

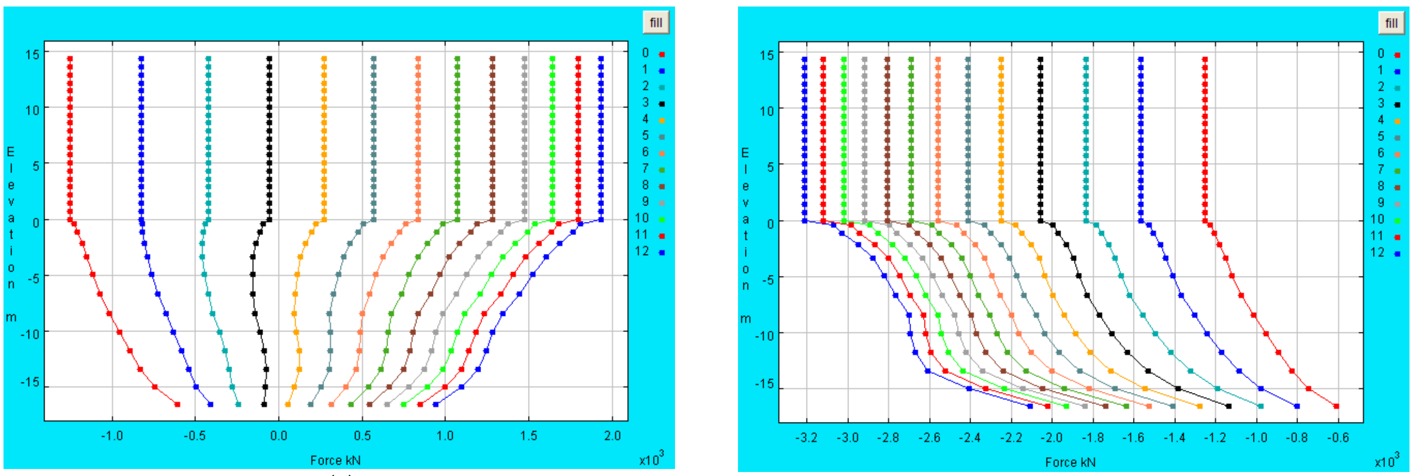

(a) (b)

Fig. 10. Axial force profile: a) Edge Central Pile # 1, and b) Edge Central Pile # 8 (see Fig. 3c for pile group layout).

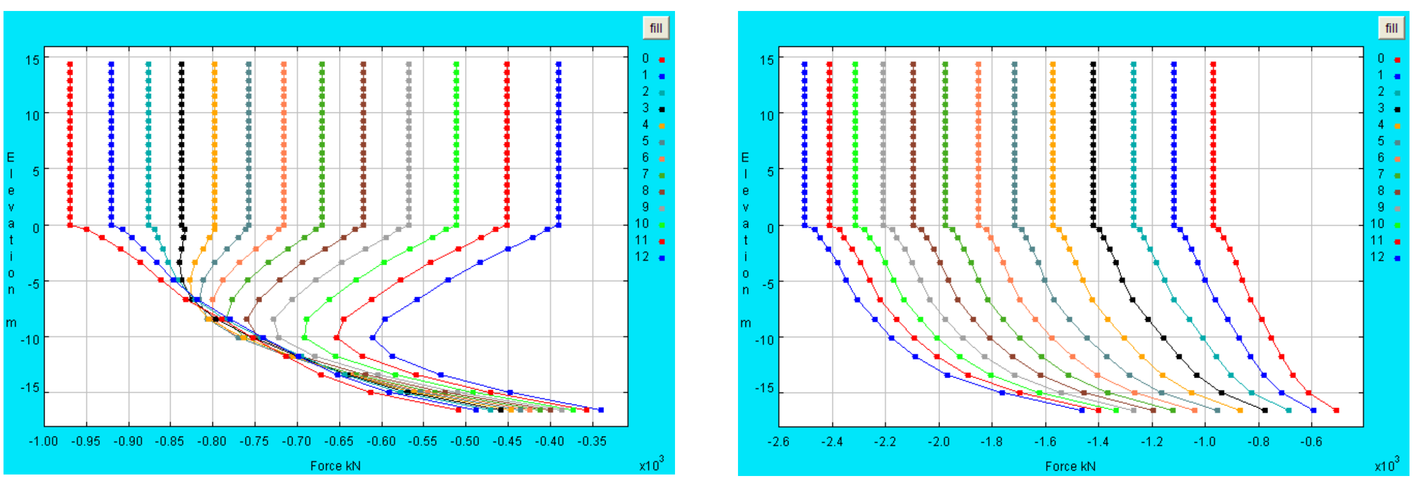

(a) (b)

Fig. 11. Axial force profile: a) Edge Pile # 11, and b) Edge Pile # 14 (see Fig. 3c for pile group layout).

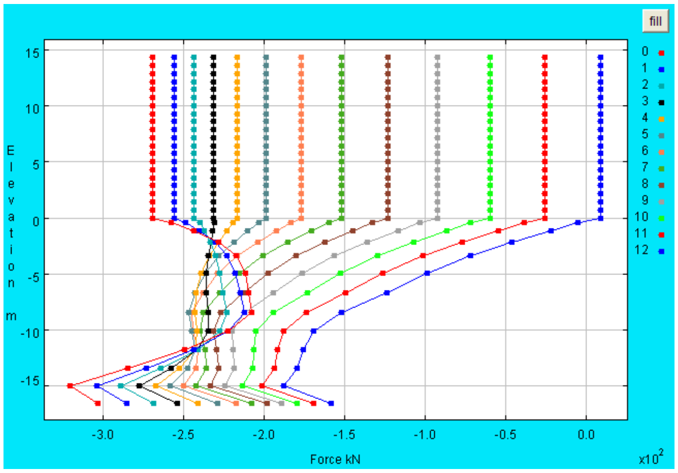

(a)

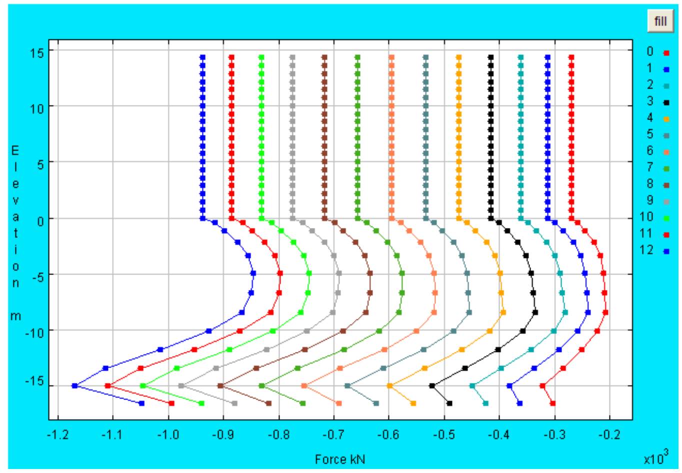

(b)

Fig. 12. Axial force profile: a)Inner Pile # 3, and b) Inner Pile # 6 (see Fig. 3c for pile group layout).

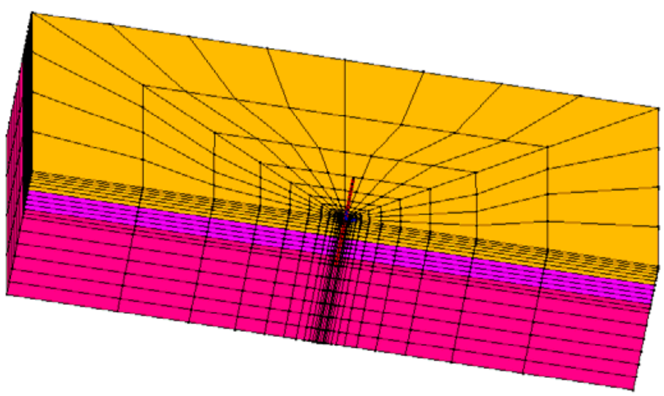

Fig. 13. Finite element mesh of the single pile model.

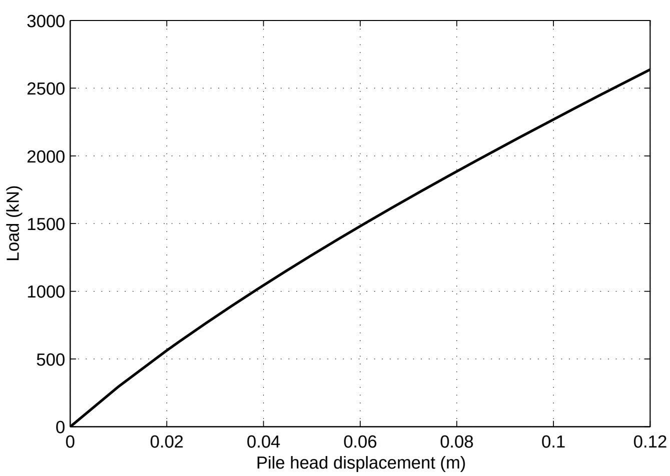

Fig. 14. Load-displacement curve for the single pile analysis

The peak longitudinal moment is 28,573 kN-m at the pile cap and -14,233 kN-m (at 3.8 m below mudline), and the peak longitudinal shear is -2,637 kN (at and above the mudline). As such, it may be noted that the single pile sustained over twice the shear and moment of the front corner pile # 16. The final deformed mesh is shown in Fig. 15, where the pattern of soil yielding may be contrasted with its pile group counterpart of Fig. 5a. In view of the close pile group spacing, the soil surrounding the pile group (Fig. 5a) exhibits a higher level of overall yielding

Loading History

At the 14.3 m elevation above the mudline, pile head displacement of up to 0.12 m was applied in 12 steps, and the response profiles are shown in Fig. 16. As noted earlier in the pile group scenario, location of peak moment and shear below the mudline moves lower with the increase in applied longitudinal displacement (due to soil yielding in the upper highly stressed strata). Evolution of the axial load transfer mechanism into the surrounding soil is also evident in Fig. 16d

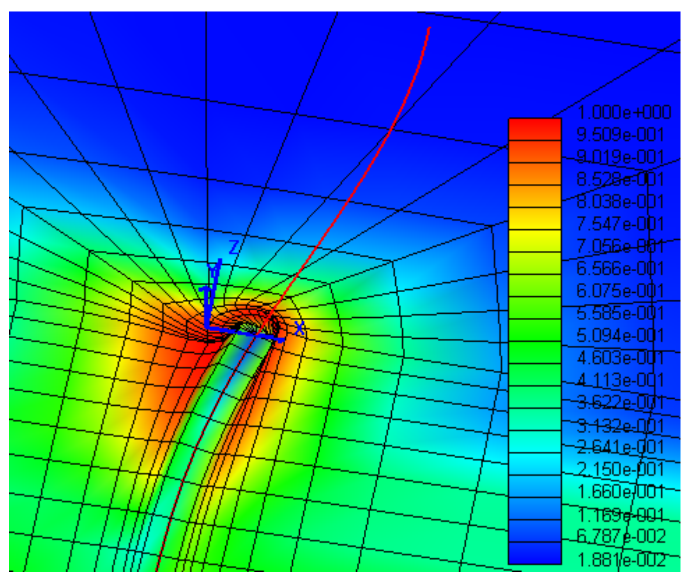

Fig. 15. Stress ratio contour fill for the single pile case at the final step (red color shows yielded soil elements; factor: 50)

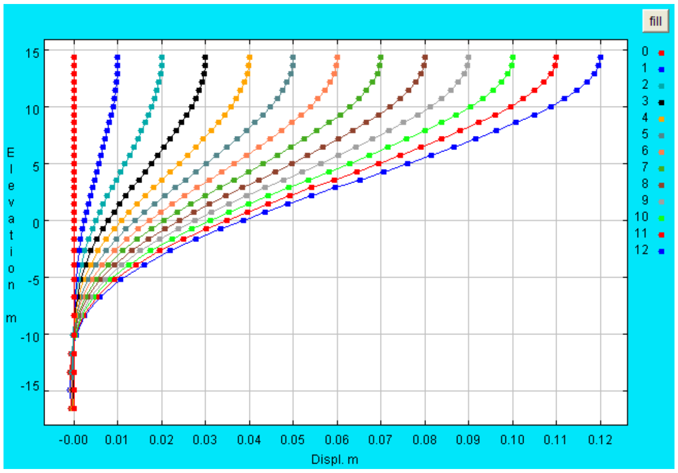

a)

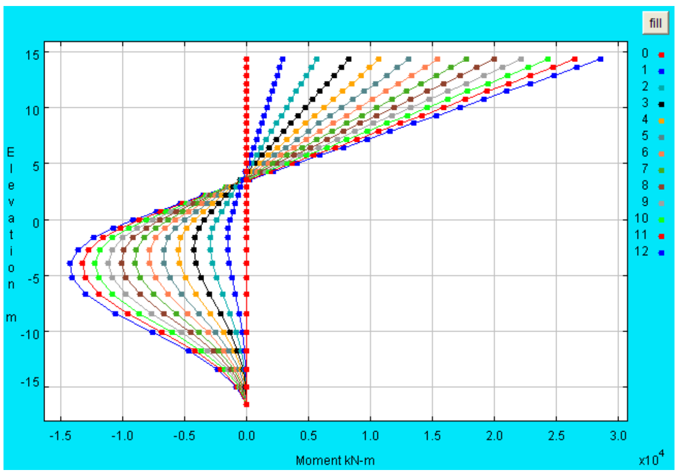

b)

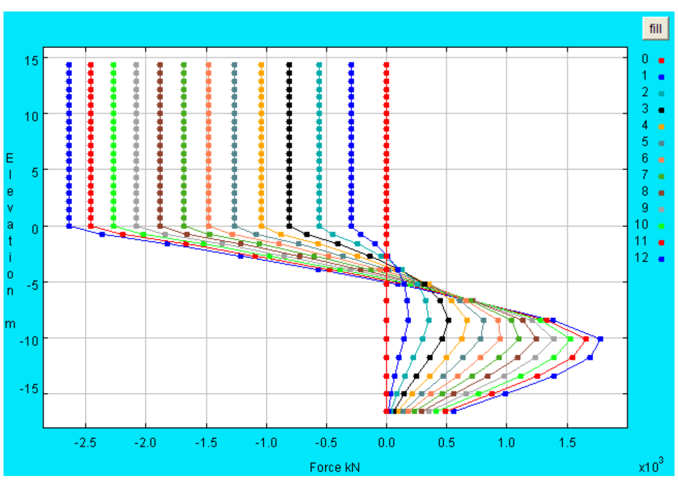

c)

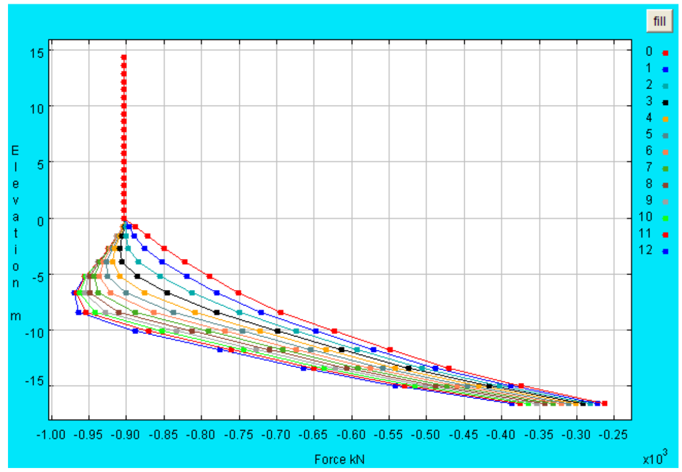

d)

Fig. 16. Response profiles for the single pile: a) longitudinal displacement; b) bending moment at the longitudinal plane; c) longitudinal shear force; d) axial force.

SOIL-PILE INTERFACE MECHANISM

In the conducted simulations, no effort was made to address the important issue of modeling the interface behavior between the soil and the pile. For instance, a gap would be expected to develop as the pile gradually moves laterally away from the adjacent soil behind it. Such mechanisms are worthy of further investigation, and stand to influence the computational simulation outcomes.

SUMMARY AND CONCLUSIONS

A pilot computational study of a large pile group system under lateral load was presented. A highly idealized linear pile response was assumed, embedded within a 3-layer stratified soil stratum represented by J_2 elasto-plastic behavior. The open-source platform OpenSees was employed throughout. The reported pre- and post-processing scenarios are generated by the user interface OpenSeesPL, a robust and versatile framework for computational analysis of pile-ground systems. Displacement in the longitudinal direction was applied to the group at the pile cap elevation. A single pile scenario was also studied for comparison. The conducted investigations aim to highlight the analysis framework capabilities and range of potential applications. Overall, the computed results indicate:

1. Corner piles carry a significantly higher proportion of the applied axial load.

2. Due to application of lateral load, back piles experience a significant reduction in axial load, resulting eventually in occurrence of tensile axial forces. Such change in axial load may adversely affect the stiffness and strength of the structural materials (reinforced concrete).

3. The front piles may have to support a substantial increase in axial compressive load, along with the imposed bending moment and shear forces.

4. With close pile spacing (of the order of 2 pile diameters), piles along the circumference of the 4x8 pile group end up carrying most of the static and dynamic loads.

5. At an equal level of applied longitudinal displacement, a large soil domain was yielded in the vicinity of the pile group, compared to the single pile scenario.

6. Additional field data and numerical/experimental investigations are needed to further refine and verify the presented analysis procedures, including the soil-pile interface characteristics, effects of pile driving/installation, mesh refinement, and nonlinear pile and soil responses.

ACKNOWLEDGMENTS

The authors are grateful for the funding provided by the Pacific Earthquake Engineering Research (PEER) Center under NSF Award Number EEC-9701568, the PEER Lifelines program, and the NSF grant No. OCI-0749227.

REFERENCES

Elgamal, A., Yang, Z., Parra, E., and Ragheb, A. 2003. Modeling of cyclic mobility in saturated cohesionless soils. *International Journal of Plasticity*, 19(6), 883-905.

Elgamal, A. Lu, J., and Forcellini, D. 2009. Mitigation of liquefaction-induced lateral deformation in a sloping stratum: 3D numerical simulation, *Journal of Geotechnical and Geoenvironmental Engineering*, 135(11), 1672-1682.

Lu, J., Yang, Z., and Elgamal, A. 2006. OpenSeesPL three-dimensional lateral pile-ground interaction version 1.00 user's manual, *Report No. SSRP-06/03*, Department of Structural Engineering, University of California, San Diego, La Jolla, CA.

Mazzoni, S., McKenna, F., and Fenves, G. L. 2006. Open system for earthquake engineering simulation user manual, Pacific Earthquake Engineering Research Center, University of California, Berkeley (http://opensees.berkeley.edu/).

Yang, Z., Elgamal, A., and Parra, E. 2003. A computational model for cyclic mobility and associated shear deformation, *Journal of Geotechnical and Geoenvironmental Engineering*, 129(12), 1119-1127.